



NOTE

# In vivo observation of lipid droplets in coral calcifying cells: fat stores to fuel the reef-building process?

Benoît Chatin<sup>1</sup> · Alexander A. Venn<sup>1</sup> ·  
Éric Tambutté<sup>1</sup> · Sylvie Tambutté<sup>1</sup>

Received: 6 April 2023 / Accepted: 14 October 2023 / Published online: 7 November 2023  
© The Author(s) 2023

**Abstract** The calcifying cells of corals are responsible for skeleton formation, a process that is the basis for reef building. Their cell biology is therefore of primary interest, but current knowledge is limited because direct in vivo investigation of this cell type is challenging. Studies at the growing edge of laterally extending coral colonies allow for direct observations of actively calcifying cells in living samples. In the current study, we used this approach to study lipid droplets, which are considered storage organelles that fuel cells for physiological processes. Using the fluorescent lipid probe Nile Red and in vivo confocal microscopy, we observed lipid droplets in calcifying cells of the coral *Stylophora pistillata* and we suggest that they play a key role in coral calcification.

**Keywords** Coral · Lipid droplets · Calcifying cell · Calicoblast · Biomineralisation · Nile Red

## Introduction

Hermatypic scleractinian corals (i.e. reef-building corals), key architects of the three-dimensional reef ecosystem framework, are lipid-rich organisms (up to 47% dry tissue weight) (Kopp et al. 2015; Stimson 1987) compared to other cnidarians, including sea anemones and jellyfishes, which display 5–20% and 1–12% dry tissue weight in lipids, respectively (Jennison 1979; Raposo et al. 2022; Revel et al. 2016). Structural lipids (e.g. membrane phospholipids)

represent 25% of coral fats, while storage lipids, mainly triglycerides and wax esters, make up 75% of this content (Patton et al. 1977). In eukaryotic cells, lipids are stored in lipid bodies, also called lipid droplets (LDs), which are considered as *bone fide* organelles (Cohen 2018). While a number of studies have investigated the roles, dynamics and composition of LDs in corals, they focused on LDs in the gastrodermis in the context of coral-dinoflagellate endosymbiosis (Chen et al. 2017, 2012; Kopp et al. 2015; Luo et al. 2009; Peng et al. 2011) and LDs in the calicodermis (calcifying epithelium) have received little attention. Yet, as key players in energy metabolism, their role in the biology of coral calcifying cells may be crucial to our understanding of the process of calcification in hermatypic corals.

The biology of coral calcifying cells at the microscopic scale is still ill-defined, partly because direct investigations in the calicodermis, sandwiched between the skeleton and overlying tissue layers, are challenging. However, there is a growing corpus of observations of subcellular processes and structures in the calicodermis, including macropinocytosis (Ganot et al. 2020), primary cilia (Tambutté et al. 2021), or pH-sensing enzymes (Barott et al. 2020). Notably, investigations at the growing edge of laterally extending coral colonies allow for direct observation of the calicodermis in living coral samples (reviewed in Venn et al. 2024, in press). In this zone of active growth, primary CaCO<sub>3</sub> crystals deposited as the first building blocks of the skeleton increase their surface by ca. 50% in a 4-h period, permitting investigations of cellular processes linked to calcification (Venn et al. 2013). In the present study, we used in vivo confocal microscopy to observe LDs in calcifying cells at the growing edge of *S. pistillata* microcolonies. Using the fluorescent lipid probe Nile Red, previously used to detect lipids in coral endodermal cells (Luo et al. 2009; Peng et al. 2011) we observed

✉ Sylvie Tambutté  
stambutte@centrescientifique.mc

<sup>1</sup> Marine Biology Department, Centre Scientifique de Monaco, 8 Quai Antoine 1er, 98000 Monaco, Monaco

lipid droplets in the calicodermis, which differ in number and size from the ones contained in the aboral gastrodermis.

## Results and discussion

The calicodermis observed at the growing edge of *S. pistillata* microcolonies displays an abundance of spherical, refringent bodies (Fig. 1A). Staining with the fluorescent lipid probe Nile Red revealed that these bodies are lipid droplets contained within calcifying cells (Fig. 1B, C). The mean density of LDs in the calcifying cells is significantly higher than in the overlying gastrodermal cell layer (respectively  $242.6 \pm 51.5/1000 \mu\text{m}^2$  versus  $30.2 \pm 8.2/1000 \mu\text{m}^2$ , mean  $\pm$  S.D.,  $n=4$ ) (Fig. 1 and Table 1). Cnidarian gastrodermal cells, which line the gastrovascular system, are involved in heterotrophic digestion, and in the case of symbiotic corals, contain endosymbiotic dinoflagellates (Symbiodiniaceae, LaJeunesse et al. 2018) responsible for autotrophic nutrition. By contrast, calcifying cells are neither in

direct contact with the coelenteric fluid nor do they contain symbiotic cells and are dependent on other epithelia for their nutrient supply. Thus, lipid droplets contained in the calicodermis likely originate from de novo, in situ synthesis inside the calcifying cells from soluble nutrients, e.g. glycerol and glucose, acquired from other cell layers (Colombo-Pallotta et al. 2010; Davy et al. 2012). Alternatively, lipids can be translocated from symbiotic cells to actively calcifying zones (Pearse and Muscatine 1971). Note that the growing edge of microcolonies contains few Symbiodiniaceae (Venn et al. 2011, Figure 1, 2024, in press), therefore lipids contained in this region probably originate from heterotrophy and/or translocation of nutrients from symbiont-rich zones. Such a transfer was observed in the branching coral *Acropora cervicornis* and in the massive coral *Orbicella annularis*, where organic compounds undergo directional transport from symbiont-rich zones to the branch tips or to the forward growing-edge, respectively, which are actively calcifying zones containing few symbionts (Taylor 1977). Interestingly, in *A. cervicornis* symbiont-free branch tips,

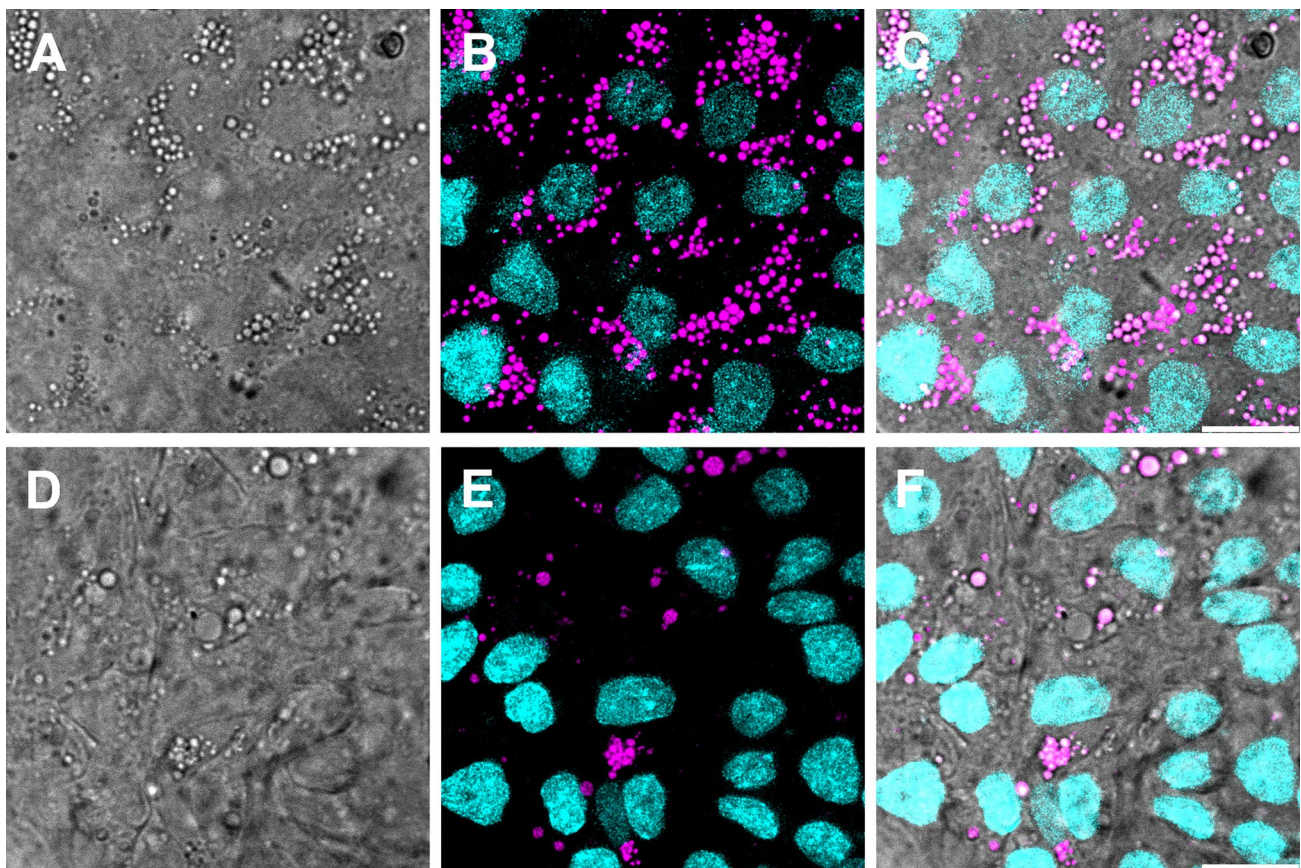


**Fig. 1** Lipid droplets observed with an inverted confocal microscope, at the growing edge of a *S. pistillata* microcolony grown on a coverslip. **A–C** Calicodermis; **D–F** aboral gastrodermis. **A, D** Transmitted light images. **B, E** confocal images displaying nuclei (cyan) and lipid droplets (magenta). **C, F** Overlay of transmitted light and confo-

cal images. Images are z projections (maximum intensity) of Z-stacks (z-step: 150 nm) acquired through the calicodermis and the aboral gastrodermis on a depth of 3.75  $\mu\text{m}$  and 6.75  $\mu\text{m}$ , respectively. Scale bars 10  $\mu\text{m}$

**Table 1** Summary of LDs characteristics observed in the calicodermis and in the gastrodermis of 4 independent *S. pistillata* microcolonies

| Colony N°    |   | 1     | 2     | 3     | 4     |                  |
|--------------|---|-------|-------|-------|-------|------------------|
| Calicodermis | LDs density/field                                   | 533   | 614   | 360   | 558   |                  |
|              | LDs density/1000 $\mu\text{m}^2$                    | 250.5 | 288.5 | 169.2 | 262.2 |                  |
|              | LDs density/1000 $\mu\text{m}^2$ (mean $\pm$ S.D.)  |       |       |       |       | 242.6 $\pm$ 51.5 |
|              | LDs Feret Minimum Diameter (colony mean) (nm)       | 756   | 743   | 717   | 790   |                  |
|              | LDs mean Feret Minimum Diameter (colony S.D.) (nm)  | 270   | 302   | 340   | 312   |                  |
|              | Diameter mean $\pm$ S.D (mean of colony means) (nm) |       |       |       |       | 752 $\pm$ 31     |
| Gastrodermis | LDs density/field                                   | 69    | 79    | 39    | 70    |                  |
|              | LDs density/1000 $\mu\text{m}^2$                    | 32.4  | 37.1  | 18.3  | 32.9  |                  |
|              | LDs density/1000 $\mu\text{m}^2$ (mean $\pm$ S.D.)  |       |       |       |       | 30.2 $\pm$ 8.2   |
|              | LDs Feret Minimum Diameter (colony mean) (nm)       | 885   | 1252  | 937   | 1099  |                  |
|              | LDs mean Feret Minimum Diameter (colony S.D.) (nm)  | 573   | 771   | 555   | 779   |                  |
|              | Diameter mean $\pm$ S.D (mean of colony means) (nm) |       |       |       |       | 1043 $\pm$ 166   |

most of the translocated organic compounds are found in the form of lipids (Pearse and Muscatine 1971). Of note, coral calcifying cells contain a large amount of mitochondria (Barott et al. 2015; Tambutté et al. 2007), which is not surprising as mitochondria and LDs are functionally linked by lipid metabolism and are often closely associated (Olzmann and Carvalho 2019).

In addition to showing differences in LDs density, comparison of LDs between the gastrodermis and calicodermis shows significative differences in size, with LDs in calcifying cells displaying a relatively narrow distribution (mean diameter  $752 \pm 31$  nm, Fig. 2A and Table 1), while gastrodermal LDs form a heterogeneous population containing large LDs ( $1043 \pm 166$  nm with some droplets up to  $4 \mu\text{m}$  in diameter, Fig. 2B and Table 1) (mean  $\pm$  S.D,  $p < 0.05$ ). These large LDs ( $> 1200$  nm) represent  $85.4 \pm 6.7\%$  of the

total LDs volume in the gastrodermis, while they account for only  $25.2 \pm 7.1\%$  of the LDs volume in the calicodermis (mean  $\pm$  S.D.). This suggests different functional roles for these two LDs pools. The small LDs observed in the calcifying cells, and to a lesser extent, in the gastrodermis present a high surface/volume ratio compared to the larger ones, allowing for increased lipid supply to cell metabolism and interaction with LD-associated proteins. By contrast, large LDs may allow lipid storage in a less easily mobilised reserve (Suzuki et al. 2011).

Taken altogether, these findings indicate that coral calcifying cells are rich in relatively small lipid droplets, suggesting an active metabolism. This is not surprising as the process of calcification is an energy-consuming process, requiring the synthesis of skeletal organic matrix (Tambutté et al. 2011) along with a transepithelial flux of ions through

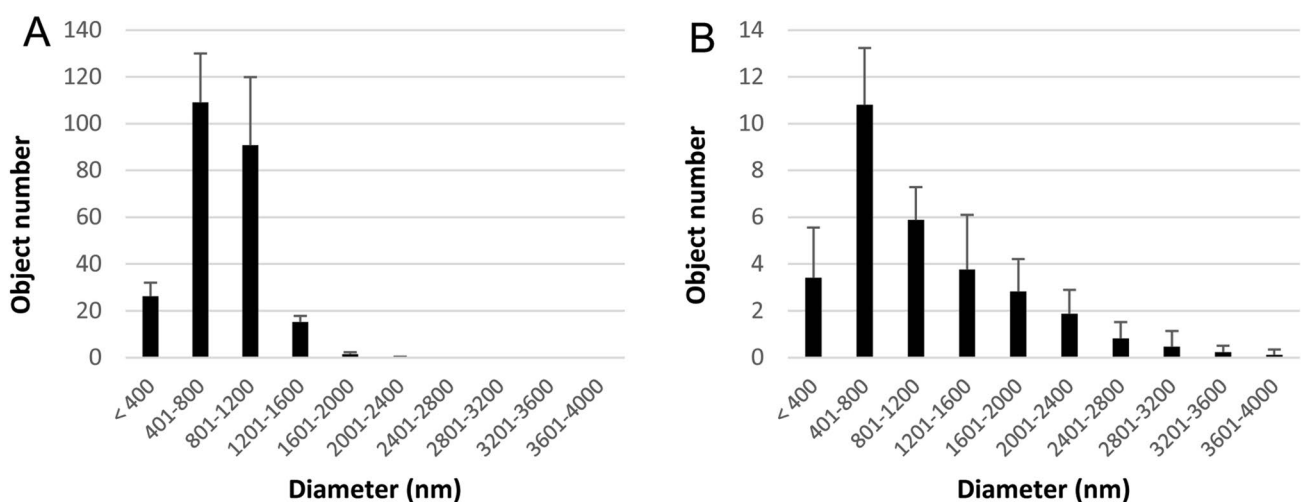


**Fig. 2** Size distribution of lipid droplets observed at the growing edge of *S. pistillata* microcolonies grown on microscope coverslips. **A** Lipid droplets size distribution in the calicodermis; **B** lipid droplets

size distribution in the aboral gastrodermis. Note that vertical scales differ between charts. Each size class represents the mean  $\pm$  S.D. of 4 independent experiments

the calicodermis to elevate and maintain the aragonite saturation state of the extracellular calcifying medium (ECM) necessary for crystal growth (Sevilgen et al. 2019; Sun et al. 2020; Venn et al. 2022). Indeed, it has been estimated that calcification represents up to 30% of coral energy budget (Allemand et al. 2011). Therefore, LDs in the calcifying cells potentially represent a metabolic energy store capable of sustaining the constant energy expenditure associated with skeletogenesis and may be essential to fuel the calcification process in periods of reduced nutrient availability. Moreover, the role of these LDs might be crucial in the context of ocean acidification (OA). For example, research by (Vidal-Dupiol et al. 2013) reports that genes involved in lipid catabolism in *Pocillopora damicornis* are upregulated under experimental OA conditions obtained through enrichment of seawater with CO<sub>2</sub>, suggesting an increase in lipid consumption at low pH. Furthermore, it was observed that in *Acropora hyacinthus*, low ECM pH is correlated with skeletal dissolution in darkness under experimental OA conditions obtained through CO<sub>2</sub> bubbling, while the OA resilient *S. pistillata*, which regulates higher pH in the ECM, is capable of maintaining calcification in the same conditions, presumably at increased energetic cost (Venn et al. 2019). A comparative study of LD abundance in the calciblastic epithelium of coral species with different OA susceptibility may shed a new light on the role of these overlooked organelles, and on their potential contribution to resilience of corals facing environmental stress.

Compared with studies where lipid abundance and metabolism were investigated at the tissue or whole-organism scale through *en masse* methods, our approach allows for the first direct observation of lipid stores in the calcifying cells of living, actively calcifying coral samples. More broadly, observation at the growing edge of LDs dynamics, along with pH regulation, crystal growth, mitochondria dynamics or other energy-related processes, under various experimental conditions, may open perspectives on the energy budget and the resilience of hermatypic scleractinian corals facing environmental stress, while providing avenues to explore the cellular biology of calcification.

## Materials and methods

### Coral samples maintenance

Experiments were conducted on *Stylophora pistillata* microcolonies laterally grown on glass coverslips in the long-term coral culture facility at the Centre Scientifique de Monaco. Aquaria were supplied with seawater from the Mediterranean Sea with an exchange rate of 50% h<sup>-1</sup>, under an irradiance of 100 μmol photons m<sup>-2</sup> s<sup>-1</sup> of photosynthetically active radiation on a 12 h:12 h light/dark cycle and at 25 °C.

Corals were fed with live *Artemia salina* nauplii twice a week, and thrice a week with frozen rotifers. Microcolonies were prepared following the lateral skeleton preparative assay (Muscatine et al. 1997; Venn et al. 2011). Briefly, flat portions (0.5–1 cm<sup>2</sup>) of *S. pistillata* mother colonies grown on glass supports were fixed with Devcon® epoxy resin on circular glass coverslips and left to grow across coverslip to a size of 1–2 cm<sup>2</sup> over 3 weeks in the culture conditions described above. Coverslips were cleaned twice a week with a razorblade to remove algae growing around the microcolony.

### Reagents

Hoechst 33342 (20 mM) was obtained from ThermoFisher. Nile red and calcein were obtained from Sigma-Aldrich. Nile red stock solution was prepared in anhydrous DMSO at 30 mM. Calcein stock solution was prepared in filtered seawater at 30 mM, and pH was adjusted at 8 with NaOH.

### Microcolony staining with fluorescent probes

Incubations of *S. pistillata* microcolonies with fluorescent probes were performed between 3:00 pm and 5:00 pm, i.e. after 7–9 h of exposure to photosynthetically active radiation but before corals daily feeding. Coral samples were incubated for 15 min in FSW containing 20 μM Hoechst 33342 and 20 μM Nile red (final DMSO concentration: 0.07%) to label nuclei and lipid droplets, respectively. Microcolonies were briefly rinsed with FSW before mounting in a microscope chamber (PeCon GmbH) containing 3 mL of FSW. Once the sample placed in the microscope and ready for imaging, FSW was replaced with FSW containing calcein at 100 μM and pH 8 to label extracellular spaces (i.e. ECM, mesoglea and coelenteron) and allow further delineation of the two aboral cell layers during image processing. Imaging was performed immediately after calcein addition.

### Microscopy

Observations were carried out at the growing-edge of *S. pistillata* microcolonies with a confocal laser scanning Leica SP8 inverted microscope monitored by the LAS X software (version 3.5.6.21594). Imaging was conducted using a 63× water immersion objective (numerical aperture: 1.2) and 4× scanner zoom. The resolution was 1024×1024 pixels and the z-step size 0.15 μm, resulting in voxels of 45 nm (x)×45 nm (y)×150 nm (z). These voxel dimensions fulfill the Nyquist-Shannon sampling criterion, as determined using the online Nyquist Calculator (SVI) tool for a 488 nm excitation wavelength and 500 nm emission wavelength. High-speed stack acquisition was performed using resonant scanner (8.000 Hz) in

**Table 2** (Materials and methods) Confocal microscope settings for fluorescent probes excitation and detection

| Probe    | Laser excitation (nm) | Laser power (%) | Detector | Detection range (nm) | Detector gain | Acquisition sequence |
|----------|-----------------------|-----------------|----------|----------------------|---------------|----------------------|
| Hoechst  | 355                   | 1               | Hybrid   | 440–470              | 400%          | Seq 2                |
| Calcein  | 488                   | 0.05            | PMT      | 500–530              | 800 V         | Seq 2                |
| Nile red | 552                   | 0.1             | Hybrid   | 560–590              | 50%           | Seq 1                |

bidirectional mode with a line averaging of 3. The pinhole size was 1 Airy Unit. The fluorescent signal from Nile red was acquired separately from Hoechst and calcein (sequential acquisition) to prevent dye crosstalk. Laser and detector settings are detailed in Table 2. Images were deconvoluted on-the-fly by the Las X-integrated Lightning tool using default parameters. In addition to fluorescence, a bright-field image was acquired using a transmitted light detector.

### Image processing and analysis

Image processing and analysis were conducted with the Las X software (Leica) including a 3D-analysis module. Image stacks were cropped to separate the calicodermis and the gastrodermis, using the calcein-stained mesoglea and Hoechst-stained nuclei as visual controls. Three-dimensional image analysis was conducted as follows: images were smoothed using a gaussian filter (radius 2.5) and thresholded using a Maximum Entropy algorithm (deviation – 750). Objects in the resultant binary image were further delineated using a morphological filter (Discard Details, radius 2) and the Split Objects tool (object size 0.5  $\mu\text{m}$  and 1.6  $\mu\text{m}$  for calicodermis and gastrodermis, respectively). LDs number, volume and minimum Feret diameter were obtained from 4 independent experiments. For LDs diameters, statistical significance was assessed with the Mann–Whitney U test using the IBM SPSS Statistics 26 software.

**Acknowledgements** The authors are grateful to Natacha Caminiti-Segonds, Nathalie Técher, Dominique Desgré, Xavier Maccario and Éric Elia for technical assistance and coral culture.

**Funding** This work was funded by the Government of the Principality of Monaco.

**Data availability** The datasets generated and analysed during the current study are available from the corresponding author on reasonable request.

### Declarations

**Competing interests** The authors declare no competing or financial interests.

**Open Access** This article is licensed under a Creative Commons Attribution 4.0 International License, which permits use, sharing, adaptation, distribution and reproduction in any medium or format, as long as you give appropriate credit to the original author(s) and the source, provide a link to the Creative Commons licence, and indicate if changes were made. The images or other third party material in this article are included in the article's Creative Commons licence, unless indicated otherwise in a credit line to the material. If material is not included in the article's Creative Commons licence and your intended use is not permitted by statutory regulation or exceeds the permitted use, you will need to obtain permission directly from the copyright holder. To view a copy of this licence, visit <http://creativecommons.org/licenses/by/4.0/>.

### References

- Allemand D, Tambutté É, Zoccola D, Tambutté S (2011) Coral Calcification, Cells to Reefs. In: Dubinsky Z, Stambler N (eds) *Coral Reefs: An Ecosystem In transition*. Springer, Dordrecht, pp 119–150. [https://doi.org/10.1007/978-94-007-0114-4\\_9](https://doi.org/10.1007/978-94-007-0114-4_9)
- Barott KL, Perez SO, Linsmayer LB, Tresguerres M (2015) Differential localization of ion transporters suggests distinct cellular mechanisms for calcification and photosynthesis between two coral species. *American Journal of Physiology-Regulatory, Integrative and Comparative Physiology* 309(3):R235–R246. <https://doi.org/10.1152/ajpregu.00052.2015>
- Barott KL, Venn AA, Thies AB, Tambutté S, Tresguerres M (2020) Regulation of coral calcification by the acid-base sensing enzyme soluble adenylyl cyclase. *Biochemical and Biophysical Research Communications* 525(3):576–580. <https://doi.org/10.1016/j.bbrc.2020.02.115>
- Chen W-NU, Kang H-J, Weis VM, Mayfield AB, Jiang P-L, Fang L-S, Chen C-S (2012) Diel rhythmicity of lipid-body formation in a coral-Symbiodinium endosymbiosis. *Coral Reefs* 31(2):521–534. <https://doi.org/10.1007/s00338-011-0868-6>
- Chen H-K, Wang L-H, Chen W-NU, Mayfield AB, Levy O, Lin C-S, Chen C-S (2017) Coral lipid bodies as the relay center interconnecting diel-dependent lipidomic changes in different cellular compartments. *Scientific Reports* 7(1), Article 1. <https://doi.org/10.1038/s41598-017-02722-z>
- Cohen S (2018) Chapter three—lipid droplets as organelles. In L Galluzzi (ed) *International review of cell and molecular biology*. Academic Press, vol 337, pp 83–110. <https://doi.org/10.1016/bs.ircmb.2017.12.007>
- Colombo-Pallotta MF, Rodríguez-Román A, Iglesias-Prieto R (2010) Calcification in bleached and unbleached *Montastraea faveolata*: Evaluating the role of oxygen and glycerol. *Coral Reefs* 29(4):899–907. <https://doi.org/10.1007/s00338-010-0638-x>
- Davy SK, Allemand D, Weis VM (2012) Cell Biology of Cnidarian-Dinoflagellate Symbiosis. *Microbiology and Molecular Biology Reviews* 76(2):229–261. <https://doi.org/10.1128/MMBR.05014-11>

- Ganot P, Tambutté E, Caminiti-Segonds N, Toullec G, Allemand D, Tambutté S (2020) Ubiquitous Macropinocytosis in Anthozoans. *eLife* 9:e50022. <https://doi.org/10.7554/eLife.50022>
- Jennison BL (1979) Annual fluctuations of lipid levels in the sea anemone *Anthopleura elegantissima* (Brandt, 1835). *Journal of Experimental Marine Biology and Ecology* 39(3):211–221. [https://doi.org/10.1016/0022-0981\(79\)90127-8](https://doi.org/10.1016/0022-0981(79)90127-8)
- Kopp C, Domart-Coulon I, Escrig S, Humbel BM, Hignette M, Meibom A (2015) Subcellular Investigation of Photosynthesis-Driven Carbon and Nitrogen Assimilation and utilization in the Symbiotic Reef Coral: *Pocillopora damicornis*. *mBio*. <https://doi.org/10.1128/mBio.02299-14>
- LaJeunesse P, Gabrielson J, Reimer V, Santos (2018) Systematic Revision of Symbiodiniaceae Highlights the Antiquity and Diversity of Coral Endosymbionts. *Current Biology* 28(16):2570–2580.e6. <https://doi.org/10.1016/j.cub.2018.07.008>
- Luo Y-J, Wang L-H, Chen W-NU, Peng S-E, Tzen JT-C, Hsiao Y-Y, Huang H-J, Fang L-S, Chen C-S (2009) Ratiometric imaging of gastrodermal lipid bodies in coral–dinoflagellate endosymbiosis. *Coral Reefs* 28(1):289–301. <https://doi.org/10.1007/s00338-008-0462-8>
- Muscatine L, Tambutte E, Allemand D (1997) Morphology of coral desmocytes, cells that anchor the calicoblastic epithelium to the skeleton. *Coral Reefs* 16(4):205–213. <https://doi.org/10.1007/s003380050075>
- Olzmann JA, Carvalho P (2019) Dynamics and functions of lipid droplets. *Nature Reviews Molecular Cell Biology* 20(3), Article 3. <https://doi.org/10.1038/s41580-018-0085-z>
- Patton JS, Abraham S, Benson AA (1977) Lipogenesis in the intact coral *Pocillopora capitata* and its isolated zooxanthellae: Evidence for a light-driven carbon cycle between symbiont and host. *Marine Biology* 44(3):235–247. <https://doi.org/10.1007/BF00387705>
- Pearse VB, Muscatine L (1971) Role of symbiotic algae (zooxanthellae) in coral calcification. *The Biological Bulletin* 141(2):350–363. <https://doi.org/10.2307/1540123>
- Peng S-E, Chen W-NU, Chen H-K, Lu C-Y, Mayfield AB, Fang L-S, Chen C-S (2011) Lipid bodies in coral–dinoflagellate endosymbiosis: Proteomic and ultrastructural studies. *Proteomics* 11(17):3540–3555. <https://doi.org/10.1002/pmic.201000552>
- Raposo A, Alasqah I, Alfheeaia HA, Alsharari ZD, Alturki HA, Raheem D (2022) Jellyfish as Food: A Narrative Review. *Foods* 11(18), Article 18. <https://doi.org/10.3390/foods11182773>
- Revel J, Massi L, Mehiri M, Boutoute M, Mayzaud P, Capron L, Sabourault C (2016) Differential distribution of lipids in epidermis, gastrodermis and hosted Symbiodinium in the sea anemone *Anemonia viridis*. *Comparative Biochemistry and Physiology Part A: Molecular & Integrative Physiology* 191:140–151. <https://doi.org/10.1016/j.cbpa.2015.10.017>
- Sevilgen DS, Venn AA, Hu MY, Tambutté E, de Beer D, Planas-Bielsa V, Tambutté S (2019) Full in vivo characterization of carbonate chemistry at the site of calcification in corals. *Science Advances* 5(1):eaau7447. <https://doi.org/10.1126/sciadv.aau7447>
- Stimson JS (1987) Location, Quantity and Rate of Change in Quantity of Lipids in Tissue of Hawaiian Hermatypic Corals. *Bulletin of Marine Science* 41(3):889–904
- Sun C-Y, Stifler CA, Chopdekar RV, Schmidt CA, Parida G, Schoeppler V, Fordyce BI, Brau JH, Mass T, Tambutté S, Gilbert PUPA (2020) From particle attachment to space-filling coral skeletons. *Proceedings of the National Academy of Sciences* 117(48):30159–30170. <https://doi.org/10.1073/pnas.2012025117>
- Suzuki M, Shinohara Y, Ohsaki Y, Fujimoto T (2011) Lipid droplets: Size matters. *Journal of Electron Microscopy* 60(suppl\_1):S101–S116. <https://doi.org/10.1093/jmicro/dfr016>
- Tambutté E, Allemand D, Zoccola D, Meibom A, Lotto S, Caminiti N, Tambutté S (2007) Observations of the tissue–skeleton interface in the scleractinian coral *Stylophora pistillata*. *Coral Reefs* 26(3):517–529. <https://doi.org/10.1007/s00338-007-0263-5>
- Tambutté S, Holcomb M, Ferrier-Pagès C, Reynaud S, Tambutté É, Zoccola D, Allemand D (2011) Coral biomineralization: From the gene to the environment. *Journal of Experimental Marine Biology and Ecology* 408(1):58–78. <https://doi.org/10.1016/j.jembe.2011.07.026>
- Tambutté E, Ganot P, Venn AA, Tambutté S (2021) A role for primary cilia in coral calcification? *Cell and Tissue Research* 383(3):1093–1102. <https://doi.org/10.1007/s00441-020-03343-1>
- Taylor D (1977) Intra-Colonial Transport of Organic Compounds and Calcium in Some Atlantic Reef Corals. <http://pascal-francis.inist.fr/vibad/index.php?action=getRecordDetail&idt=PASCAL7850225407>
- Venn A, Tambutté E, Holcomb M, Allemand D, Tambutté S (2011) Live Tissue Imaging Shows Reef Corals Elevate pH Under Their Calcifying Tissue Relative to Seawater. *PLOS ONE* 6(5):e20013. <https://doi.org/10.1371/journal.pone.0020013>
- Venn AA, Tambutté E, Holcomb M, Laurent J, Allemand D, Tambutté S (2013) Impact of seawater acidification on pH at the tissue–skeleton interface and calcification in reef corals. *Proceedings of the National Academy of Sciences* 110(5):1634–1639. <https://doi.org/10.1073/pnas.1216153110>
- Venn AA, Tambutté E, Caminiti-Segonds N, Techer N, Allemand D, Tambutté S (2019) Effects of light and darkness on pH regulation in three coral species exposed to seawater acidification. *Scientific Reports* 9(1):2201. <https://doi.org/10.1038/s41598-018-38168-0>
- Venn AA, Tambutté E, Comeau S, Tambutté S (2022) Proton gradients across the coral calcifying cell layer: Effects of light, ocean acidification and carbonate chemistry. *Frontiers in Marine Science*. <https://doi.org/10.3389/fmars.2022.973908>
- Venn AA, Tambutté E, Zoccola D, Capasso L, Allemand D, Caminiti-Segonds N, Techer N, Ganot P, Tambutté S (2024) Coral calcification at the cellular scale: Insight through the ‘window’ of the growing edge. In *Frontiers in Invertebrate Physiology*. ISBN 9781003403319
- Vidal-Dupiol J, Zoccola D, Tambutté E, Grunau C, Cosseau C, Smith KM, Freitag M, Dheilily NM, Allemand D, Tambutté S (2013) Genes Related to Ion-Transport and Energy Production are Upregulated in Response to CO<sub>2</sub>-Driven pH Decrease in Corals: New Insights from Transcriptome Analysis. *PLOS ONE* 8(3):e58652. <https://doi.org/10.1371/journal.pone.0058652>

**Publisher’s Note** Springer Nature remains neutral with regard to jurisdictional claims in published maps and institutional affiliations.